RELATIONSHIP ANALYSIS BETWEEN FOREST ABOVEGROUND BIOMASS AND VEGETATION INDICES USING SENTINEL-2 DATA

Tsolmon Altanchimeg[1], Amarsaikhan Damdinsuren[1], Tsolmon Renchin[2], Dorjsuren Chimidnyam[3]
[1]Institute of Geography and Geoecology, Mongolian Academy of Sciences
[2]Department of Physics, National University of Mongolia
[3]Institute of Botanical Garden, Mongolian Academy of Sciences
Email: tsolmon_a@mas.ac.mn

KEYWORDS: Forest aboveground biomass, linear regression model, vegetation indices

ABSTRACT: The forest is a very important natural resource that plays a significant role in keeping an environmental stability, ecological balance, environmental conservation, water quality protection, maintenance of wildlife habitat, wilderness and open space preservation, food security and sustainable development in all nations. Forest aboveground biomass plays a pivotal role in the carbon cycle and climate change mitigation in the ecosystem. In addition, it is an important parameter in forest management and estimation of volume/ capacity of forest resources. The aim of this study is to investigate the relationship between estimated forest aboveground biomass and spectral indices derived from visible and infrared bands of multichannel Sentinel-2 satellite data. For correlation analysis between the vegetation indices and spectral data to estimate aboveground biomass in boreal forest, regression models are applied. The study area is Teshig soum of Bulgan aimag and is located in northern part of Mongolia and belongs to a forest-steppe eco-region. To calculate the aboveground biomass in sampling plots, forest stand parameters such as diameter at breast height (DBH) and tree height (H) have been measured, and allometric equations were used. In the final analysis, we studied the relationship between the aboveground biomass measured at sampling plots and vegetation indices.

1. INTRODUCTION

Forests cover about one-third of the world's land surface, but alone generate nearly half of net primary products and store more than 80% of terrestrial plant carbon. Forests play a special role in protecting, regulating water, improving water quality, and protecting soil from erosion and degradation. Forests and cultivated forests will increase rainfall and moisture supply in the area and create favorable microclimate conditions. Forests increase air precipitation by 5-15%, dew and frost by 30-40% (Ellison, et al., 2017; Karl, et al., 2009). Mongolia's total forested area or forest fund consists of 18.6-million-hectare areas which are 11.8 % of total land area (FRDC, 2021).

Nowadays, to determine and monitor forest biomass, and conduct research on the environment and natural resources, researchers are effectively using remote sensing (RS) images with different spatial and spectral characteristics along with various types of accurate ground-measured and thematic datasets. Over the years, the multispectral information has been extensively used to forecast and assess the properties of different vegetation types. Leaf area, biomass, chlorophyll content, plant height, and plant stress are identified by various plant-related vegetation indices (Chappelle, et al., 1992). Vegetation indices are mathematical transformations of spectral reflectance values used to describe biomass and vegetation coverage (He et al., 2006). This is a value which quantifies the reflectance of the spectral bands to take into account the evolution of the vegetation per pixel of an aerial image.

Spectral reflectance is used to understand the nature of plant characteristics, but affected by various factors such as plant structure, soil properties, atmospheric conditions, topography, and moisture content (Pinter, Jr, et al., 2003). Vegetation absorption for spectral bands is high from 0.7 µm, and until 1.3 µm, but depends on the internal structure of plant. However, between 1.35 µm and 2.5 µm, the internal structure of the leaf will still have some effect, but the water contained in the leaf will play an important role in energy absorption. As the plant matures, it begins to lose its high reflectance in the near-infrared spectrum, and as it matures, pigments other than chlorophyll begin to predominate, at which point the plant loses its green color and becomes yellowish or reddish-yellow (Damdinsuren, 2019; Ray, 1994). The study used field measurements data of 2018 and the Sentinel-2 optical dataset.

In this research, we aimed to determine the relationship between the above-ground biomass (AGB) of the forest and the vegetation indices estimated from the Sentinel-2 satellite multispectral data. The specific objectives of the research are: 1) To estimate the maximum biomass of forest land; 2) To calculate vegetation indices from multispectral sensor; 3) To calculate the relationship between vegetation indices and ABG of forest land.

2. DATA SOURCES

A sample plot is composed by nested circles with radius of 20 meter (Figure 1). Regeneration counted in 3 height classes: Measurement of standing trees diameter at breast height (DBH) 6-14 cm in 6-meter radius, DBH 15-25.9 cm

12 meter radius and DBH>30 cm 20 radius, respectively. We used methodology of Mongolian multipurpose National Forest inventory. Before measuring the distance and angle of bearing between the center of the circle and the center of the tree. It is also possible to determine the health, cause of damage, quality, degree of decay or biomass loss of trees counted in the sampling area. The diameter of the chest height is measured at a height of 1.3 meters above grade.

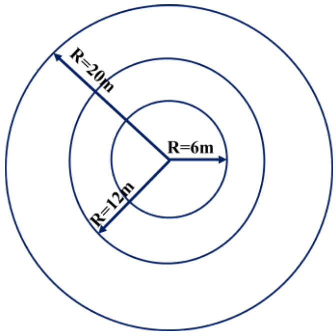

Figure 1. Plot area.

Sentinel-2 is a new generation of multispectral satellite imagery that has been launched on 23 June 2015 by the European Space Agency (ESA). It has 13 spectral bands with 3 different spatial resolutions (10, 20, and 60 meter). The three 60 meter bands (bands 1, 9, and 10), which are mainly focused on cloud screening and atmospheric correction and a wide swath of 290 km, a radiometric resolution of 12 bits, and 5 days of revisit times by two satellites (Drusch, et al., 2012).

3. STUDY AREA AND METHODOLOGY

The study area is Teshig soum located in Bulgan province, and situated 250 km away from the province center. The study was distributed over an area about 7719 square.km and elevation was between 1560-1820 meters above the sea level, and has a harsh and extreme climate. The study area has the largest mountain plateau, and 88% of the total territory is covered with forests, and includes the Khargal lake (Figure 2). The territory of soum is mountainous, the largest lake of Bulgan province is located, and 88% of the total territory is covered with forests. Air temperature rise and fall to +36˚C in the summer and -49˚C in the winter. The mean annual temperature is -2.4˚C, and mean annual precipitation range is between 250-300mm.

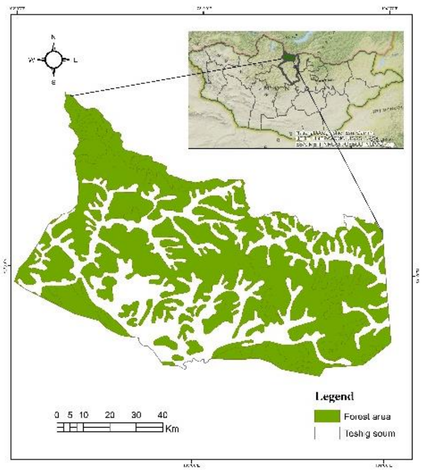

Figure 2. Study area.

The allometric models were derived based on the relationship between above ground biomass (AGB) and diameter at breast (DBH) and total height of tree (H_{tot}^{c}) measurements.

$$AGB = a * DBH^{b} * H_{tot}^{c} \quad (1)$$

Where: Above ground biomass (AGB) (tonnes), (dry biomass of stem, branch and leaves)
DBH – Tree diameter (m) (1,3 м)
Htot – Tree total height (m)
a – Species specific factor
b - Species specific DBH exponential factor

c - Species specific Htot exponential factor.

The allometry equations species-specifics coefficients different from for each tree species.

We used 35 vegetation indices, such as the ratio of near-infrared and red channels, the ratio of red-green light channels, the ratio of red light and near-infrared channels, and the ratio of near-infrared and blue channels and they were calculated from the bands of the Sentinel-2 dataset.

Table 1. The used vegetation indices.

1	ATSAVI x=0.08 a=1.22 b=0.03	$a\frac{NIR - aRED - b}{aNIR + RED - a*b + x(1+a^2)}$	Adjusted Transformed Soil Adjusted Vegetation	(Broge & Leblanc, 2001)
2	GNDVI	$\frac{NIR - GREEN}{NIR + GREEN}$	Green Normalized Difference Vegetation Index	(Gitelson & Merzlyak, 1998)
3	NDVI	$\frac{NIR - RED}{NIR + RED}$	Normalized Difference Vegetation Index	(Sellers , et al., 1994)
4	SAVI	$\frac{NIR - RED}{(NIR + RED + L)(1 + L)}$	Soil Adjusted Vegetation Index	(Huete, 1988)
5	SLAVI	$\frac{NIR}{RED + SWIR}$	Specific Leaf Area Vegetation Index	(Lymburner, et al., 2000)
6	VARVI	$\frac{GREEN - RED}{GREEN + NIR + RED}$	Visible Atmospherically Resistant Index	(Gitelson, et al., 2002)
7	ARVI	$\frac{NIR - RED - y*(RED - BLUE)}{NIR + RED - y*(RED - BLUE)}$	Atmospherically Resistant Vegetation Index	(Bannari, et al., 1995)
8	WDRVI	$\frac{0.1NIR - RED}{0.1NIR + RED}$	Wide Dynamic Range Vegetation Index	(Ahamed, et al., 2011)
9	RGR	$\frac{RED}{GREEN}$	Simple Ratio Red- Green ration	(John & Surfus, 1999)
10	IO	$\frac{RED}{BLUE}$	Simple Ration Red/Blue Iron Dioxide	(Hewson, et al., 2001)
11	DVI	$\frac{NIR}{RED}$	Simple Ration/Difference Vegetation Index	(Tucker, 1979)
12	GRV	$\frac{NIR}{G}$	Simple Ration/Green Ratio Vegetation Index	(Sripada, et al., 2005)
13	BSI	$\frac{(SWIR + R) - (NIR - B)}{(SWIR + R) + (NIR + B}$	Soil Bareness Index	(Rasul, et al., 2018)
14	SIPI	$\frac{NIR - BLUE}{NIR - RED}$	Structure Insensitive Pigment Index	(Penuelas, et al., 1995)
15	NORM G	$\frac{G}{NIR + RED + G}$	NORM G	(Henrich & Brüser, n.d.)
16	EVI	$2.5*\frac{NIR - RED}{(NIR + 6RED - 7.5BLUE) + 1}$	Enhanced Vegetation Index	(Huete, et al., 2002)
17	CI	$\frac{RED - BLUE}{RED}$	Coloration index	(Bannari, et al., 2016)
18	CIgreen	$\frac{NIR}{GREEN} - 1$	Chlorophyll Index Green	(Ahamed, et al., 2011)
19	FI	$\frac{2R - G - B}{G - B}$	Shape Index	(Henrich & Brüser, n.d.)
20	LAI	3.618*EVI-0.118	Leaf Area Index	(Boegh, et al., 2002)
21	SR	$\frac{P_{nir}}{P_{red}}$	Ratio Vegetation Index/ Simple ratio	(Birth & McVey, 1968)
22	CVI	$NIR\frac{RED}{GREEN^2}$	Chlorophyll Vegetation Index	(Datt, et al., 2003)
23	IPVI	$\frac{\frac{NIR}{NIR + RED}}{2}*(NDVI + 1)$	Infrared percentage vegetation index	(Crippen, 1990)
24	MSAVI	$\frac{2*NIR + 1 - \sqrt{(2*NIR + 1)^2 - 8*(NIR - RED)}}{RED}$	Modified Soil Adjusted Index	(Qi, et al., 1994)

25	MSR NIR/RED	$\frac{\left(\frac{NIR}{RED}\right)-1}{\sqrt{\left(\frac{NIR}{RED}\right)+1}}$	Modified Simple Ratio NIR/RED	(Chen & Cihlar, 1996)
26	RDVI	$\frac{800nm-670nm}{(800nm+670nm)^2}$	Re-normalized Difference Vegetation Index	(Roujean & Breon, 1995)
27	SQRT	$\sqrt{\frac{NIR}{RED}}$	SQRT(IR/R)	(Henrich & Brüser, n.d.)
28	TDVI	$\left(0.5+\frac{(NIR-RED)}{(NIR+RED)^2}\right)^{0.5}$	Transformed Vegetation Index	(Bannari , et al., 2005)
29	TVI	$0.5*\left(120*\frac{(NIR-GREEN)}{(NIR+GREEN)}\right)$	Triangular Vegetation Index	(Broge & Leblanc, 2001)
30	VARI	$\frac{NIR-RED}{(NIR+RED-BLUE)}$	Visible Atmospherically Resistant Vegetation Index	(Gitelson, et al., 2002)
31	GBNDVI	$\frac{NIR-(GREEN+BLUE)}{NIR+(GREEN+BLUE)}$	Green-Blue NDVI	(Wang, et al., 2007)
32	GLI	$\frac{2*NIR-RED-BLUE}{2*NIR+RED+BLUE}$	Green Leaf Index	(Gobron, et al., 2000)
33	NDGI	$\frac{NIR-GREEN}{NIR+GREEN}$	Normalized Difference Glacier Index	(Keshri, et al., 2009)
34	GARI	$\frac{NIR-(GREEN-(BLUE-RED))}{NIR-(GREEN+(BLUE-RED))}$	Green Atmospherically Resistant Vegetation Index	(Gitelson, et al., 1996)
35	NDWI	$\frac{NIR-SWIR}{NIR+SWIR}$	Normalized Difference Water Index	(Gao, 1996)

4. RESULTS AND DISCUSSION

Linear regression analysis is used to establish the relationship between quantitative parameters. The correlation analysis is a method for calculating the influence of these parameters on one another. Regression correlation analysis is inextricably related and it is a widely considered requirement prior to any linear regression analysis. As a result, a compairing correlation analysis was conducted to examine the relationship between VIs and AGB field measured data.

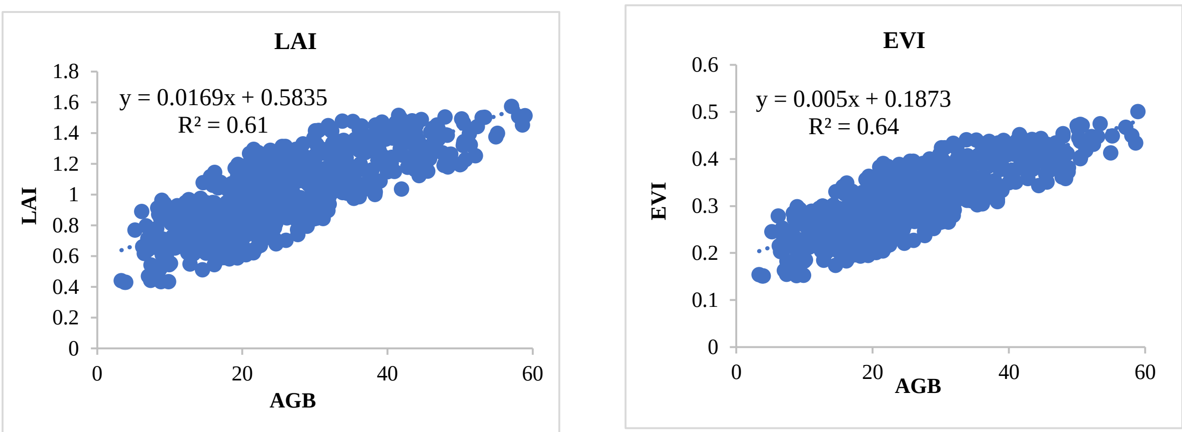

Figure 3: a. Relationship between LAI and AGB b. Relationship between EVI and AGB

In the study, measurements were performed in 641 sampling areas. Thus, vegetation indices and AGB derived from Sentinel-2 satellite data were estimated using a linear regression model. We used regression to forecast quantitative and continuous values. A t-statistic was used to determine whether linear regression model parameters were statistically significant. Of the 35 indices used in this study, the Leaf Area Index (LAI) was statistically significant with the p value ($p \leq 0.003$) and the Enhanced Vegetation Index (EVI) ($p \leq 0.0001$) were highly correlated with AGB.

Table 2. Determination coefficients of Vis and AGB.

№	Variable	R2	№	Variable	R2
1	ATSAVI	0.01	18	FI	0.01
2	GNDVI	0.1	19	SR	0.59
3	NDVI	0.57	20	CVI	0.001
4	SAVI	0.57	21	IPVI	0.57
5	SLAVI	0.17	22	MSAVI	0.56
6	VARVI	0.003	23	MSR NIR/RED	0.58
7	ARVI	0.013	24	RDVI	0.51
8	WDRVI	0.0	25	SQRT	0.04
9	RGR	0.01	26	TDVI	0.57
10	IO	7e09	27	TVI	0.1
11	DVI	0.05	28	VARI	0.24
12	GRV	0.03	29	GBNDVI	0.02
13	BSI	0.11	30	GLI	0.03
14	SIPI	0.0001	31	NDGI	0.02
15	NORM G	0.03	32	GARI	0.41
16	CIgreen	0.03	33	NDWI	0.18
17	CI	0.02			

Vegetation indices calculated from satellite data are used to estimate vegetation cover and they indicate vegetation greenness. Vegetation index models use wavelengths in the electromagnetic spectrum of green vegetation to determine vegetation characteristics. Vegetation indices were determined using multispectral data. AGB had a good relationship with the leaf area index (LAI) (R^2=0.61) and enhanced vegetation index (EVI) (R^2=0.64), respectively. In addition, NDVI, SAVI, IPVI and TDVI indices were correlated (R^2=0.57), SR (R^2=0.59), MSAVI (R^2=0.56), MSR (R^2=0.58), RDVI (R^2=0.51), and GARI (R^2=0.41), respectively.

5. CONCLUSIONS

RS is the most useful tool to estimate the biomass over large regions. The vegetation index should be a good indicator of vegetation cover, excluding soil background and other effects. Thirty-five VIs were applied in this study, which were calculated based on the reflectance of the top canopy. We intended to observe the relationship between the estimated AGB and VIs in the study area. In this research, vegetation cover density was calculated by different vegetation indices to discriminate vegetated areas using multispectral channels to study distribution. The vegetation reflects high in the NIR spectral band and has strong absorption in the visible red spectral bands. Moreover, it measures the greenness and health of vegetation from satellite images. A significant relationship was found between the AGB and certain vegetation indices. As seen from the study, AGB had the highest relationships with the LAI and EVI and those vegetation indices are suitable to estimate AGB of the boreal forest area in Mongolia.

ACKNOWLEDGEMENT

This research was supported by scholarship named after scientist Ochir Gonchig. We thank to Mongolian Geospatial Association for the useful comments.

REFERENCES

Amarsaikhan, D., 2019. *Principles of Modern Geographic Information Systems and RS. Erdem Press,* Mongolian Academy of Sciences, pp.264.

Ahamed, T., Tian, L., Zhang, Y. & Ting, K., 2011. A review of remote sensing methods for biomass feedstock production. *Biomass and Bioenergy,* 35(7), pp. 2455-2469.

Ahamed, T., Tian, L., Zhang, Y. & Ting, K., 2011. A review of remote sensing methods for biomass feedstock production. *Biomass and Bioenergy,* 35(7), pp. 2455-2469.

Bannari , A. A., Asalhi, H. & Teillet, P. M., 2005. Transformed difference vegetation index (TDVI) for vegetation cover mapping. *IEEE International Geoscience and Remote Sensing Symposium,* pp. 3053-3055.

Bannari, A. et al., 2016. Assessment of Land Erosion and Sediment Accumulation Caused by Runoff after a Flash-Flooding Storm Using Topographic Profiles and Spectral Indices. *Advances in Remote Sensing*, 5(4), pp. 315-354.

Bannari, A., Morin, D., Bonn, F. & Huete, A. R., 1995. A review of vegetation indices. *Remote sensing reviews,* 13(1-2), pp. 95-120.

Birth, G. S. & McVey, G. R., 1968. Measuring the Color of Growing Turf with a Reflectance Spectrophotometer. *Agronomy journal,* 60(6), pp. 640-643.

Boegh, E. et al., 2002. Airborne multispectral data for quantifying leaf area index, nitrogen concentration, and photosynthetic efficiency in agriculture. *Remote Sensing of Environment,* 81(2-3), pp. 179-193.

Broge, N. H. & Leblanc, E., 2001. Comparing prediction power and stability of broadband and hyperspectral vegetation indices for estimation of green leaf area index and canopy chlorophyll density. *Remote Sensing of Environment,* 76(2), pp. 156-172.

Broge, N. H. & Leblanc, E., 2001. Comparing prediction power and stability of broadband and hyperspectral vegetation indices for estimation of green leaf area index and canopy chlorophyll density. *Remote Sensing of Environment,* 76(2), pp. 156-172.

Chappelle, E. W., Kim, M. S. & McMurtrey III, J. E., 1992. Ratio analysis of reflectance spectra (RARS): An algorithm for the remote estimation of the concentrations of chlorophyll A, chlorophyll B, and carotenoids in soybean leaves. *Remote Sensing of Environment,* 39(3), pp. 239-247.

Chen, J. M. & Cihlar, J., 1996. Retrieving leaf area index of boreal conifer forests using Landsat TM images. *Remote Sensing of Environment,* 55(2), pp. 153-162.

Crippen, R. E., 1990. Calculating the vegetation index faster. *Remote Sensing of Environment,* 34(1), pp. 71-73.

Datt, B. et al., 2003. Preprocessing EO-1 Hyperion hyperspectral data to support the application of agricultural indexes. *IEEE Transactions on Geoscience and Remote Sensing,* 41(6), pp. 1246 - 1259.

Drusch, M. et al., 2012. Sentinel-2: ESA's Optical High-Resolution Mission for GMES Operational Services. *Remote Sensing of Environment,* Volume 120, pp. 25-36.

Ellison, D. et al., 2017. Trees, forests and water: Cool insights for a hot world. *Global Environmental Change,* Volume 43, pp. 51-61.

FRDC, 2021. *Report of the Forest Fund of Mongolia,* Ulaanbaatar: Forest research and development center.

Gao, B.-c., 1996. NDWI—A normalized difference water index for remote sensing of vegetation liquid water from space. *Remote Sensing of Environment,* 58(3), pp. 257-266.

Gitelson, A. A., Kaufman, Y. J. & Merzlyak, M. N., 1996. Use of a green channel in remote sensing of global vegetation from EOS-MODIS. *Remote Sensing of Environment,* 58(3), pp. 289-298.

Gitelson, A. A., Kaufman, Y. J., Stark, R. & Rundquist, D., 2002. Novel algorithms for remote estimation of vegetation fraction. *Remote Sensing of Environment,* 80(1), pp. 76-87.

Gitelson, A. A. & Merzlyak, M. N., 1998. Remote sensing of chlorophyll concentration in higher plant leaves. *Advances in Space Research,* 22(5), pp. 689-692.

Gobron, N., Pinty, B., Verstraete, M. & Widlowski, J.-L., 2000. Advanced vegetation indices optimized for up-coming sensors: Design, performance, and applications. *IEEE Transactions on Geoscience and Remote Sensing,* 38(6), pp. 2489 - 2505.

Henrich,V.&Brüser,K.,n.d.*indexdatabase.de.*[Online] Available at: https://www.indexdatabase.de/

Hewson, R., Cudahy, T. & Huntington, J., 2001. *Geologic and alteration mapping at Mt Fitton, South Australia, using ASTER satellite-borne data.* Sydney, IEEE, pp. 2939-2941.

He, Y., Guo, X. & Wilmshurst, J., 2006. Studying mixed grassland ecosystems I:suitable hyperspectral vegetation indices. *Canadian Journal of Remote Sensing,* 32(2), pp. 98-107.

Huete, A. R., 1988. A soil-adjusted vegetation index (SAVI). *Remote Sensing of Environment,* 25(3), pp. 295-309.

Huete, A. R. et al., 2002. Overview of the radiometric and biophysical performance of the MODIS vegetation indices. *Remote Sensing of Environment,* 83(1-2), pp. 195-213.

John , G. & Surfus, J. S., 1999. Assessing leaf pigment content and activity with a reflectometer. *New Phytologist,* 143(1), pp. 105-117.

Karl, T. R., Melillo, J. M. & Peterson, T. C., 2009. *Global Climate Change Impacts in the United States,* New York: Cambridge University Press.

Keshri, A. K., Shukla, A. & Gupta, R. P., 2009. ASTER ratio indices for supraglacial terrain mapping. *International Journal of Remote Sensing,* 30(2), pp. 519-524.

Lymburner, L., Beggs, P. J. & Jacobson, C. R., 2000. Estimation of Canopy-Average Surface-Specific Leaf Area Using Landsat TM Data. *Photogrammetric Engineering and Remote Sensing,* pp. 183-191.

Penuelas, J. et al., 1995. Reflectance assessment of mite effects on apple trees. *International Journal of Remote Sensing,* 16(14), pp. 2727-2733.

Pinter, Jr, P. J. et al., 2003. Remote Sensing for Crop Management. *Photogrammetric Engineering & Remote Sensing,* Volume 69, p. 647–664.

Qi, J. et al., 1994. A modified soil adjusted vegetation index. *Remote Sensing of Environment,* 48(2), pp. 119-126.

Rasul, A. et al., 2018. Applying Built-Up and Bare-Soil Indices from Landsat 8 to Cities in Dry Climates. *Land,* 7(3), pp. 1-13.

Ray, T. W., 1994. A FAQ on Vegetation in Remote Sensing. *Vegetation indices in Remote Sensing* , pp. 1-18.

Roujean, J.-L. & Breon, F.-M., 1995. Estimating PAR absorbed by vegetation from bidirectional reflectance measurements. *Remote Sensing of Environment,* 51(3), pp. 375-384.

Sellers , P. J. et al., 1994. A global 1° by 1° NDVI data set for climate studies. Part 2: The generation of global fields of terrestrial biophysical parameters from the NDVI. *International Journal of Remote Sensing* , 15(17), pp. 3519-3545.

Sripada, R. P., Heiniger, R. W., White, J. G. & Weisz, R., 2005. Aerial Color Infrared Photography for Determining Late-Season Nitrogen Requirements in Corn. *Agronomy Journal,* 97(5), pp. 1443-1451.

Tucker, C. J., 1979. Red and photographic infrared linear combinations for monitoring vegetation. *Remote Sensing of Environment,* 8(2), pp. 127-150.

Wang, F.-m., Huang, J.-f., Tang, Y.-l. & Wang, X.-z., 2007. New Vegetation Index and Its Application in Estimating Leaf Area Index of Rice. *Rice Science,* 14(3), pp. 195-203.